Hemicelluloses hydrogel: Synthesis, characterization, and application in dye removal

C.A. Rodríguez-Ramírez, Joana E. Tasqué, Nancy Lis Garcia, Norma B. D'Accorso

PII: S0141-8130(23)03907-7

DOI: https://doi.org/10.1016/j.ijbiomac.2023.127010

Reference: BIOMAC 127010

To appear in: *International Journal of Biological Macromolecules*

Received date: 17 April 2023

Revised date: 14 August 2023

Accepted date: 18 September 2023

Please cite this article as: C.A. Rodríguez-Ramírez, J.E. Tasqué, N.L. Garcia, et al., Hemicelluloses hydrogel: Synthesis, characterization, and application in dye removal, *International Journal of Biological Macromolecules* (2023), https://doi.org/10.1016/j.ijbiomac.2023.127010

Hemicelluloses hydrogel: synthesis, characterization, and application in dye removal

C.A. Rodríguez-Ramírez [a,c], Joana E. Tasqué [b], Nancy Lis Garcia [c] and Norma B. D'Accorso [a,c*]

[a] Universidad de Buenos Aires, Departamento de Química Orgánica, Facultad de Ciencias Exactas y Naturales, Buenos Aires, Argentina.

[b] YPF Tecnología (Y-TEC), Berisso, Argentina.

[c] CONICET- Universidad de Buenos Aires. Centro de Investigaciones en Hidratos de Carbono (CIHIDECAR). Buenos Aires, Argentina.

Abstract

Novel materials using biowaste as adsorbents in wastewater treatment have been allocated considerable interest. Herein, we present the synthesis of different hydrogels of crosslinked polyacrylamide in presence of hemicelluloses with/ without bentonite, using a soft reaction condition. The structure of new hydrogels was characterized by spectroscopic, thermal and microscopic experiments. The semi-interpenetrated network with hemicelluloses: 10 %; acrylamide 79 %; bentonite 10 %; *N,N,N′,N′*-tetramethylethylenediamine: 1 % allows reducing 20 % the use of non-renewable acrylamide, without changing its decomposition temperatures and keeping its water absorption capacity. This hydrogel was applied to dye removals, such as rhodamine B, methylene red and methylene blue in aqueous solutions. In the case of methylene blue, highest removal is observed with maximum adsorption of q_{max}= 140.66 mg/g, compared to material without hemicelluloses that only a q_{max}= 88.495 mg/g. The adsorption kinetics and equilibrium adsorption isotherms are in accordance with the pseudo-second-order kinetic model and Langmuir isotherm model, respectively. The developed hydrogel from hemicelluloses represents a potential alternative adsorbent for a sustainable system of sewage treatment.

Keywords. Hemicelluloses, Polysaccharide, Adsorption, Dyes, Wastewater, Hydrogel.

* Corresponding author. Tel./fax: +54 11 4576 3346. E-mail address: norma@qo.fcen.uba.ar (N.B. D'Accorso). C. A. Rodriguez Ramirez and J. E. Tasque contributed equally to this work and are co-first authors.

Introduction

Water is the most essential and valuable natural resource on Earth. This natural resource has a vital role in preserving the quality of life and ecology. However, only 0.3% of the total amount of water is fresh water. The limited availability and inadequate use of fresh water make it impossible to satisfy the demands of the existing population. Among the main factors that have generated this increase in world demand for water consumption is the increase in world population, changes in consumption patterns, the expansion of agricultural irrigation and increases in living standards [1,2].

Water pollution is enlisted as one of the most exasperating problems that require an instant and realistic solution, in the opposite case, it would become a serious threat to sustainable environmental development. According to data collected by United Nations, every day around 2 tons of artificial garbage are dumped negligently into our rivers and streams [3]. The main source of contamination of these natural sources is produced by the discharge of unprocessed industrialized and non-industrialized effluents such as dyes, pesticides, heavy metals, and organic and inorganic pollutants [4].

Dyes are organic compounds that impart color to a substrate. Annually, about 700,000 tons of various dyes are produced and used in many products in the textile, cosmetic, pharmaceutical, plastics, food packaging, paint, paper, and leather industries [5,6]. Inefficient dyeing operations and untreated effluents generate alterations in the ecological conditions of aquatic life. The impact includes decreased light penetration through the water, which directly affects photosynthesis in aquatic plants, causing oxygen deficiency. In addition, these organic compounds have been shown a mutagenic, teratogenic and carcinogenic effects in humans. Some of these effects are adjudicated to DNA damage, jaundice, nausea, cyanosis, mental confusion and shock. Therefore, its disposal from wastewater becomes an essential objective for environmental remediation and public health [7].

Organic dyes are characterized by having complex structures that make their degradation difficult, generating challenges in the extraction processes. In this context, numerous technologies have been developed and experimented with for

treating colored industrial effluents. Among these, physicochemical methods have been widely employed, encompassing flocculation, precipitation and advanced chemical oxidation [8,9]. Despite their effectiveness, these methods suffer from certain limitations, including the production of sludge, high operational and reagent costs, and the formation of soluble by-products,, which are often more toxic [9]. Therefore, adsorption methods emerge as one of the most attractive, practical and low-cost solutions to remediate water contaminated with dyes.

Hydrogels are three-dimensional (3D) networks of crosslinked hydrophilic polymers that can absorb large amounts of water into the structure. However, conventional synthetic polymer hydrogels are typically not biodegradable. In this way, the exploration of new hydrogels composed of biomaterials with low environmental impact, such as polysaccharides isolated from renewable sources. The use of polysaccharides from biowaste emerges as a new class of cutting-edge materials with a wide range of applications, especially the elimination of organic dyes in the environment [7,10].

In literature is described different routes to improve the strength and modulus of hydrogels, that including hydrogel reinforcement using organic/inorganic fibers or particles as well as the design of composites hydrogels [11–13]. A type of said composite networks can be created by the simultaneous or sequential cross-linking of at least two polymer networks in combination. The result of such syntheses are dense polymeric alloys made of interlaced macromolecular networks that are collectively known as semi interpenetrating polymer networks (semi-IPN) [14].

After cellulose, hemicelluloses (HC) are the most abundant renewable biological resource produced by plants, representing a very promising resource. Currently, there is a growing interest in its recovery and transformation into functional products for use in different applications. Possible chemical modifications of HC create new opportunities to exploit their diverse properties [1]. It is important to note that the presence of hydroxyl and carboxyl groups allow the formation of covalent and non-covalent bonds, resulting in being very attractive for the preparation of different materials of industrial interest [15].

On the other hand, it is important to note that bentonite (BT) exhibits interesting properties, such as being a natural clay with high abundance, low cost, and excellent adsorbent properties. Based on these characteristics, BT has been utilized in various wastewater treatment applications [14,15]. This material is primarily based on montmorillonite, which is made up of two silicon oxygen tetrahedron clip a layer of alumina 2:1 type of octahedral crystal structure [18]. The presence of Si-O and O-H bonds on the surface of BT can interact with copolymer chains and generate 3D structure [19].

Respect to organic polymers, the polyacrylamide (PAM) and their copolymers have found interesting applications in the biomedical field as well as in remediation processes [20,21]. The presence of amine groups in the chain, allows the interaction with inorganic and organic compounds, by hydrogen bonds.

Bentonite is an important mineral clay due to its environmental and economic relevance. The incorporation of clay materials, such as bentonite, can enhance the adsorption prowess of hydrogels. Nevertheless, the powdered nature of this adsorbent poses a challenge in terms of its recovery from liquid phases, primarily due to the limited practicality of conventional filtration or centrifugation techniques. This limitation curtails its potential applications across various industrial contexts. As a result, dedicated research endeavors have been channeled into integrating clay materials into diverse 2D and 3D structures [22,23].

Taking into account the considerations described above, and to the best of our knowledge the combined of organic polymers and inorganic products in presence of biopolymers to obtain three-dimensional networks capable to dyes adsorption has not yet been reported. Therefore, the purpose of this work is twofold: to enhance the synergistic effect of crosslinked acrylamides and bentonite in the presence of hemicellulose from an endemic bamboo (Tacuara cane) to synthesize a structural hydrogel and to analyze their ability adsorption and remove industrial dyes in water.

2. Materials and methods

2.1 Materials

The hemicelluloses (HC) were isolated from Tacuara Cane. Samples were collected in April 2021 from City Tigre located in Buenos Aires Argentina. The cane was cut and dried in an oven for 24 h at 45 °C. Acrylamide (Am, 99 %), *N*, *N*-methylenebisacrylamide (BIS, 99 %), Ammonium persulfate (APS, 98 %), bentonite (BT), *N,N,N′,N′*-tetramethylethylenediamine (TEMED, 99 %), and methanol (MeOH) were purchased from Sigma Aldrich. All reagents were used as received without further purification. The chemical products (toluene, ethanol, NaOH and HCl) used to extract the HC were of analytical quality from Sigma-Aldrich. Rhodamine B (Rh B), methylene blue (MB) and methylene red (MR) were purchased from Sigma-Aldrich. Deionized water was used in all experiments and the preparation of the aqueous solutions.

2.2 Extraction of hemicelluloses

In a previous work we described the isolation and characterization of different component of Tacuara Cane [24,25]. In **Figure 1** the simplified procedure is shown, where the HC were obtained in around 21% respect of the cane mass**.**

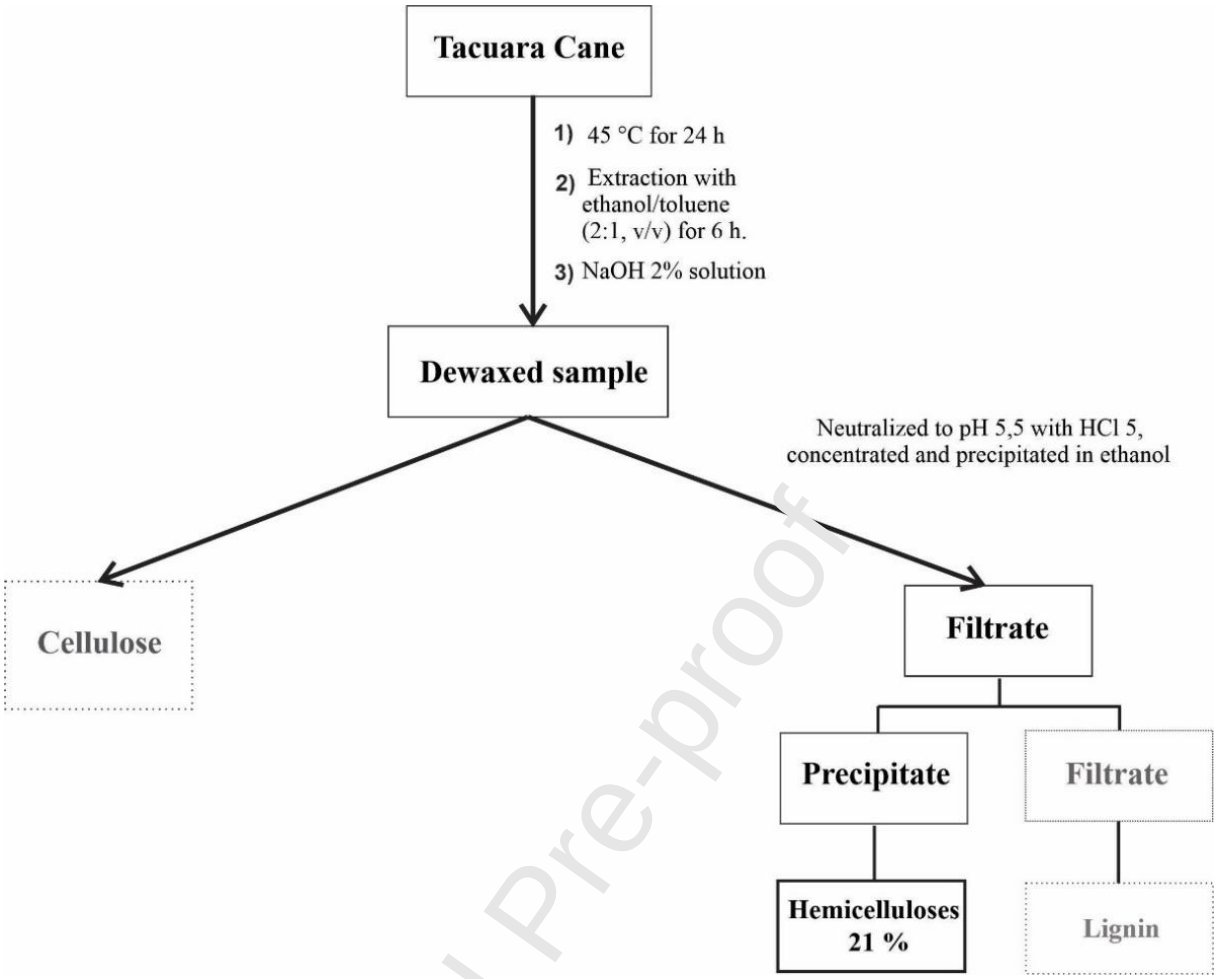

Figure 1. Simplified procedure for the extraction of HC.

2.3. Synthesis of HC-g-Am BIS-BT

Hydrogels were prepared by free radical graft copolymerization of HC and Am in the presence of BIS as crosslinking agent, and a redox initiator system (APS/TEMED). HC (0.1 g) was dissolved in aqueous solution of NaOH 0.2 % (5 mL) at 25 °C for 1 h with constant stirred. Then Am, APS, BIS and BT were added in the proportion shown in Table **1**, the system was purged with argon for 20 min. Then, TEMED (0.1 g) was added, the redox initiator started. The reaction mixture was kept for 3 h. Finally, the resulting material was filtered and washed with methanol. The solvent was removed under reduced pressure. The white final solid was immersed in water for 48 h. The remaining water was extracted to remove the residual monomer. Then, the hydrated material was dried at 40 °C until complete water extraction.

The criterion applied for the experimental design of the different samples was to vary the amounts of HC and BT in the Am-BIS system. The amount of BIS was later reduced.

Table 1. The reaction conditions for the preparation of semi-IPN.

Samples	BIS (%)	BT (%)	HC (%)	Am (%)
Am-BIS	5	0	0	95
HC-g-Am-BIS	5	0	10	85
Am-BIS-BT	5	10	0	85
HC-g-Am-5-BIS-BT	5	10	10	75
HC-g-Am-2.5-BIS-BT	2.5	10	10	77.5
HC-g-Am-1-BIS-BT	1	10	10	79
Am-1-BIS-BT	1	10	0	89

2.4 Characterization

2.4.1 Fourier- transform Infrared Spectroscopy (FTIR-ATR)

Fourier-transform infrared spectra were recorded on a Nicolet IS50 in attenuated total reflectance mode (FTIR-ATR) with a diamond crystal. The frequency range used for measured were between 500- 4000 cm^{-1}, employing 32 scans and a resolution of 4 cm^{-1}.

2.4.2 Proton Nuclear Magnetic Resonance (^{1}H NMR)

The hydrogel was characterized by ^{1}H NMR spectrum on a Bruker NMR spectrometer at 300 MHz at 25 °C. The semi-IPN sample (20 mg) was dissolved in deuterium oxide (D_2O). The proton spectrum was realized with water suppression and recorded after 128 scans.

2.4.3 Thermogravimetric analysis

Thermogravimetric analysis (TGA) was carried out on a TGA-51 Shimadzu thermogravimetric analyzer. The temperature range used for the analysis of the samples were between 25 to 850 °C at a heating rate of 5 °C/min using a nitrogen flux rate was 30 cm^3/min.

2.4.4 Field Emission Scanning Electron Microscopy (FESEM)

The surface morphology of prepared hydrogels of HC-g-Am-BIS-BT and Am-BIS-BT were observed by scanning electron microscope Zeiss Supra 40 with a field emission gun operated at 2 kV. Swollen hydrogels were freeze-dried before cutting and the surface of the sections was put up sputtered coated with a thin layer of gold before observation.

2.4.4 Water absorbency measurement

Through gravimetric method swelling experiments were conducted using distillate water at room temperature. The swollen hydrogels were removed from the solutions, wiped with filter paper, and then weighed as soon as possible. The tests of all samples were conducted in triplicate. The swelling ratio (S) at the time (t) was calculated as follows Eq (1):

$$S = \frac{W_t - W_d}{W_d} \quad (1)$$

where the term Wt is the weight at time t during the swelling process and Wd is the initial weight of the dry hydrogel.

2.4.5 Adsorption thermodynamics and kinetics studies

2.4.5.1 Adsorption kinetics

Kinetic studies were performed at 25 °C and pH 7 using approximately 0.05 g of HC-g-Am-BIS-BT and Am-BIS-BT and 5 mL of MB solution (400 mg/L) with a contact time of 10–60 min. To determine the controlling mechanism of the adsorption process, the experimental kinetic data were then fitted through three kinetic models, including pseudo-first order, pseudo-second order Eqs (8) and (9) respectively.

$$\log(q_e - q_t) = \log q_e - K_1 t \quad (8)$$

$$\frac{t}{q_t} = \frac{1}{K_2 q_e^2} + \frac{1}{q_e} t \quad (9)$$

where qt (mg/g) is the adsorption capacity at time t (min), and K_1 (1/min) and K_2 (g/mg.min) are the rate constants of the PFO and PSO models, respectively.

2.4.5.2 Dye adsorption studies

The adsorption of MB, Rh B and MR from aqueous solutions onto HC-g-Am-BIS-BT and Am-BIS-BT were systematically estimated. Before the adsorption experiments, a stock solution of MB at 700 mg/L, Rh B 700 mg/L and MR with 50 mg/L were prepared by dissolving an accurately weighed amount of the powder in deionized water. In is important to remark that the different between the concentrations used is due to the low solubility of MR in water [26]. Then absorbance was measured by using a UV/Vis spectrophotometer (Jenway 6705 spectrophotometer) which recorded the characteristic absorption peak each dye: MB at wavelength of 664 nm, Rh B at 554 nm and MR at 430 nm [27]. A calibration curve was constructed in relation to absorbance values of the corresponding concentration dyes. The adsorption capacities q_e (mg/g) were assessed using **Eq. 2.**

$$q_e = \frac{(C_o - C_e)V}{m} \quad (2)$$

where C_o and C_e are the initial and equilibrium concentrations of MB (mg/L), respectively, m is the adsorbent mass (g) and V is the MB solution volume (L).

On the other hand, Eq (3) was utilized to estimate the MB dye removal capacity and removal efficiency (%), respectively.

$$Dye\ removal\ (\%) = \frac{100(C_o - C_e)}{C_o} \quad (3)$$

To identify the adsorption behavior, the MB dye was chosen. The experimental data of MB concentration of the solutions before (50 –2000 mg/L) and after dye removal in the equilibrium were used to interpret four adsorption models: The Langmuir Eq. (4), Freundlich Eq. (5) and Temkin Eq. (6) isotherms equation are given:

$$\frac{C_e}{q_e} = \frac{1}{K_L q_m} + \frac{C_e}{q_m} \quad (4)$$

$$Ln\ q_e = Ln\ K_F + \frac{1}{n}\ Ln\ C_e \quad (5)$$

$$q_e = B_T InK_T + B_T InC_e \quad (6)$$

The parameter in Eq 3-5, C_e (mg/L) corresponding and equilibrium concentration of MB in solution, q_e (mg/g) is the amount of adsorbed MB at equilibrium. For the case of the isotherm of Langmuir, q_m (mg/g) is defined how the maximum monolayer coverage adsorption capacity, while Langmuir coefficient K_L (L/mg) is related to adsorption energy. On the other hand, q_m and K_L values can be estimated from the slope obtained by plotting C_e/q_e vs C_e, resulting in a linear relationship, since q_m and K_L can be determined from the slope $1/q_m$ and intercept $1/ (q_m K_L)$, respectively.

Freundlich model (K_F) and (n) related to the capacity and intensity of adsorption, respectively. Likewise, K_F and indicator 1/n are obtained by plotting ln q_e against Ln (C_e). On the other hand, in the Temkin isotherm B_T ($J.mol^{-1}$) is the constant that is controlled by temperature, as K_T (L/g) is the binding constant of Temkin isotherm. The values of B and K_T constants were obtained from the slope and intercept achieved by plotting q_e against ln C_e.

Another parameter studied using the Langmuir isotherm was dimension less separation factor (RL):

$$R_L = \frac{1}{1 + K_L C_O} \quad (7)$$

The calculated values of R_L were found to be favorable during the whole range of dye concentration (100-400 mg/L).

2.4.5.3 Reusability studies

HC-g-Am-BIS-BT (0.1 g) was immersed into 100 mL of MB dye solution (400 mg/L) with constant stirring during 60 min at 30 °C. After the adsorption equilibrium, the MB dye loaded hydrogel samples were separated from the solution by filtration and the samples were dried completely. MB-loaded hydrogels were treated with 100 mL of HCl solution (0.1 M) for 60 min, with the objective to desorb the MB dye. Then, the semi-IPN network was subsequently washed with distilled water several times.

2.4.5.4 BET analysis

Textural characterization of the samples was carried out from the determination of the N2 adsorption isotherms at 77 K, using an automatic Micromeritics ASAP 2020 HV. Prior to the analysis, the samples were degassed for 2 hours at 348 K under a flow of He. The conventional BET procedure was applied in order to evaluate the specific surface area (SBET). The total pore volume (Vt) was calculated from the volume of N2 absorbed at the maximum relative pressure (P/Po= 0.99). The average pore diameter was calculated from: Dmp= 4Vt/SBET. The pore size distribution (PSD) was determined from the isotherms using the density functional theory (DFT) method applying the Micromeritics DFT Plus software.

3. Results and discussion

3.1 Preparation and structure of semi-IPN hydrogels

The semi-IPN hydrogels were prepared by grafting copolymerization of Am, onto HC chains in presence of BIS as a crosslinking agent and powdery BT. APS and TEMED were used as redox initiators for polymerization. The mechanism for the hydrogel preparation is shown in **Figure 2**.

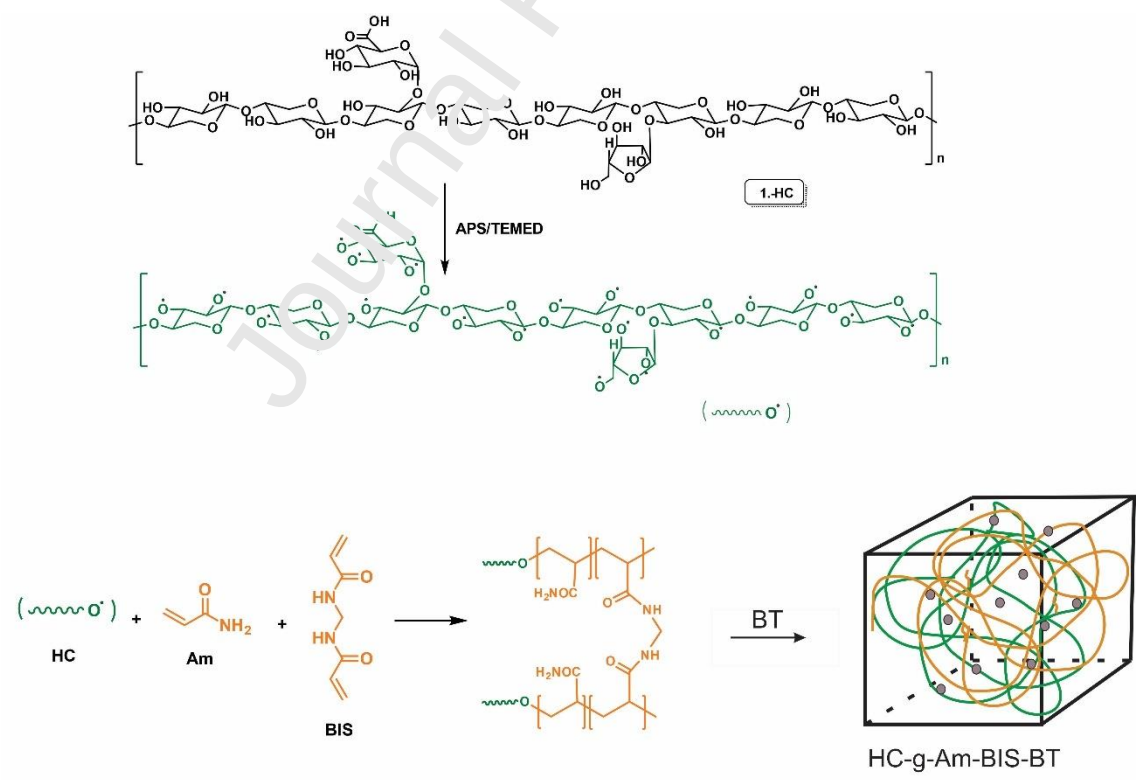

Figure 2. Proposed reaction mechanism for HC-g-Am-BIS-BT hydrogels.

Many articles describe the mechanism of graft copolymerization in polysaccharides such as cellulose [28,29], starch [30] and chitosan [31] via free radical to obtain semi-IPNs. Briefly, sulfate anion radical was generated from $(NH_4)_2S_2O_8$ under heating. These radical abstracts hydrogen from the hydroxyl group of the HC backbone to form alkoxy radicals. After active center on the HC backbone, the Am monomer and BIS become acceptors started graft polymerization. The presence of BIS and BT produces the crosslinked structure, which formed the tridimensional network.

3.2 Characterization

The chemical structure of HC-g-Am-BIS-BT hydrogels can be confirmed by infrared spectroscopy. FTIR-ATR spectra of the HC, BT and crosslinked BIS (Am-BIS) are shown in **Figure 3**.

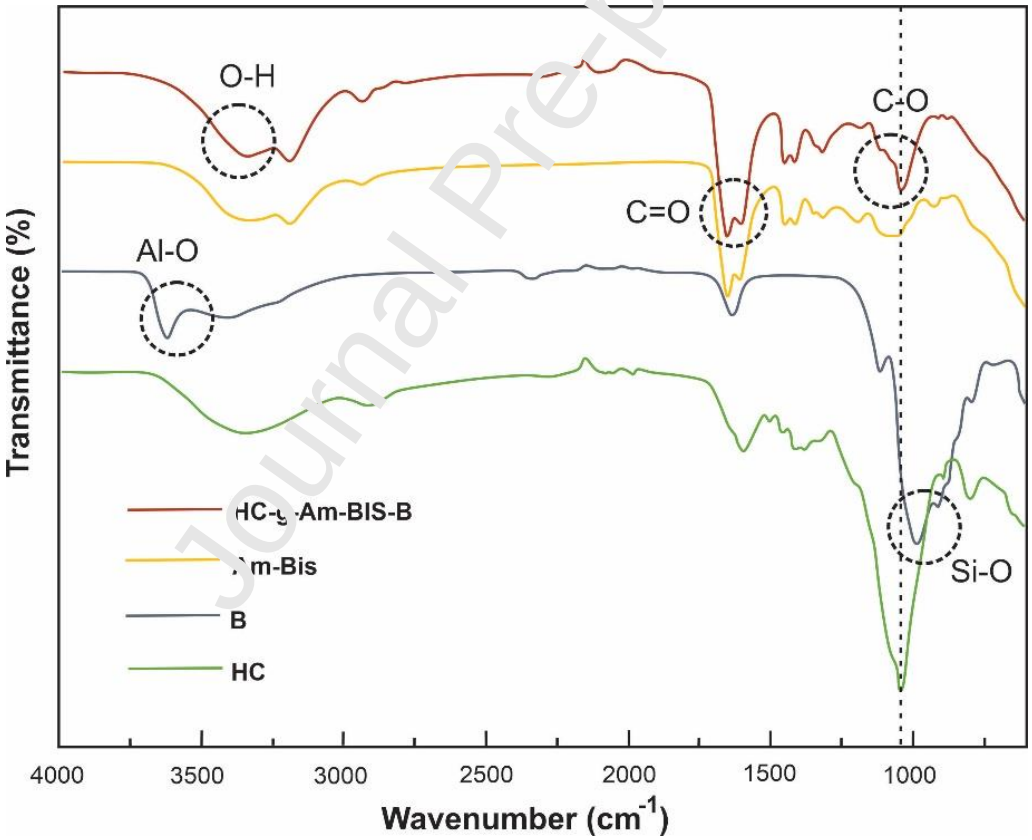

Figure 3. FT-IR spectra of hemicelluloses (HC), hydrogels (HC-g-Am-BIS-BT), Am-BIS and bentonite (BT).

The initial unmodified HC (green line) showed the typical signals previously reported in literature to hemicellulose obtained from other renewable sources [32]. Briefly, the representative signals were the stretching of vibration of the O-H

bonds that is observed around 2990-3700 cm^{-1}. Similarly, at 2913 cm^{-1} CH stretching was evident [33]. Furthermore, the bands were observed between 1000 cm^{-1} and 1200 cm^{-1} are the typical presence of 4-*O*-methylglucuronoxylans [34].

On the other hand, BT (blue line) presented the peaks at 3630 cm^{-1} and 3431 cm^{-1} were attributed to the O-H (Al-OH) and O-H stretching respectively. The band at 1645 cm^{-1}, was assigned to O-H bending. Besides, the broad and intense peak at 1040 cm^{-1} was ascribed to the Si-O stretching, while the bands at 790 cm^{-1} and 524 cm^{-1} were consistent with the classical signals of Si-O-Al stretching and Si-O-Al bending vibrations respectively [35–38].

The Am-BIS (orange line) and HC-g-Am-BIS-BT (red line) spectrum, showed a broad band around 3342 cm^{-1} and a characteristic peak at 3215 cm^{-1} due to the stretching vibrations of N-H. The significant characteristic peaks at 1651 and 1606 cm^{-1} could be attributed to the carbonyl stretching vibration and N–H bending vibration of the amide group, respectively [39–41]. It is important to remark that, HC-g-Am-BIS-BT spectrum exhibited an additional band at 1050 cm^{-1} consisting with C-O-C stretching attributed at glycosidic linkages. Similar results were reported in xylans and HC, which is a confirmation that HC play a part in the crosslinking reaction [42].

In addition, NMR characterization was performed**.** In **Figure 4** is shown the ^{1}H-NMR spectrum of HC-g-Am-BIS-BT.

The signals of the crosslinked Am-BIS units were identifiable as two broad signals: the first signal at around of 1.6 ppm, which was attributed to methylene from the polymeric chain, while the signal at 2.2 ppm arises from the response of the methine protons from the polymeric chain. The characteristic peaks stemming from the HC backbone can be observed between 3.2-4.2 ppm [43]. The presence of these signals allows us to affirm that there is a covalent interaction between the hemicellulose and the acrylic monomers [44]. Besides, from this spectrum is determined the residual monomer and it is important to remark that the residual monomer is less than 0.1 %.

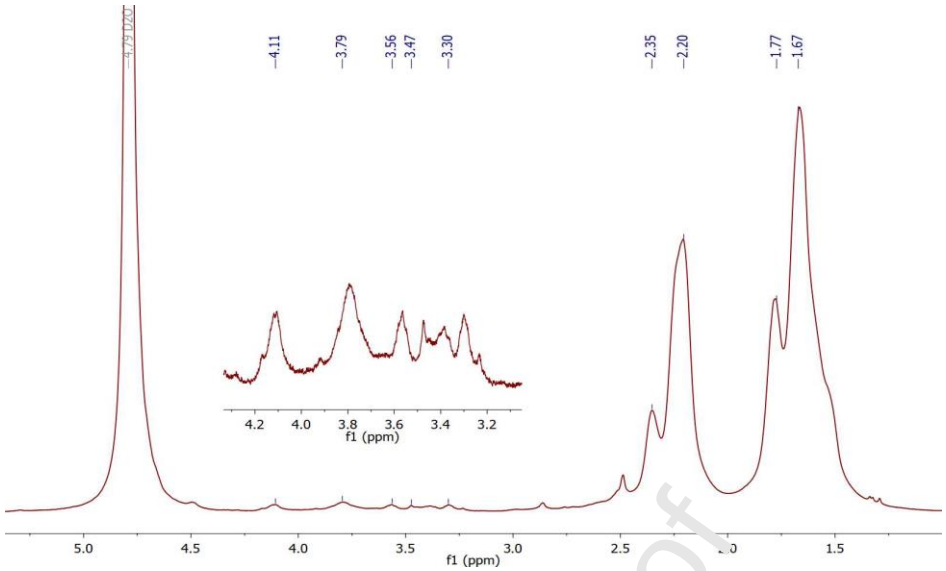

Figure 4. ^{1}H NMR spectrum of HC-g-Am-BIS-BT (200 MHz, D_2O).

Regarding the thermal characterization of the materials, it is shown in **Figures 5A** and **B** the TGA (% mass loss) and DTG curves for HC, hydrogels and the product without HC.

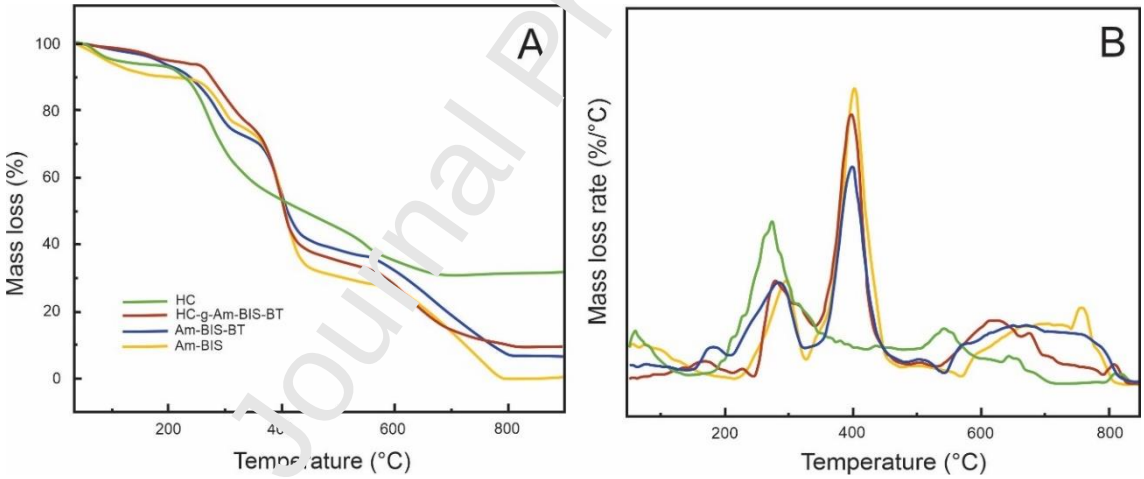

Figure 5. **A**:TGA, and **B**: DTG the of HC and modified HC and hydrogels.

In the first stage between 50 to 200 °C, all samples showed a clear weight loss caused by water remaining within the different structures. However, HC-g-Am-BIS-BT showed in this stage the lowest mass loss, that can be attributed to an increase in the hydrophobicity due to the grafting of Am and BIS onto the HC backbone.

In the second stage to 200-600 °C, the HC showed a loss of ~50 % caused by the pyrolysis and depolymerization of the xylans in its structure [45]. For Am-BIS, the degradation in the second stage is due to a deamination reaction manifested by

the loss of ammonia gas from amide groups of polyacrylamide (PAM) chains [28]. However, Am-BIS-BT shows an increase in its decomposition temperature when compared to Am-BIS. This behavior was similar to the results reported by Nakason *et al* 2010, who observed a beneficial effect in increasing the decomposition temperature of the materials in which BT was incorporated [37,46]. BT provides rigidity to the system because it offers potential attachment points with the hemicellulose matrix. On the other hand, the incorporation of BT in semi-IPN increases the strength of a superabsorbent polymer through the formation of new ester bonds [47,48].

Finally, in the third stage (more than 600°C), HC showed a residual weight of 30.1 % due mainly to carbonaceous residues formation in the inert atmosphere and the inorganic compounds formed during its isolation [49]. The amounts of solids presented by HC-g-Am-BIS-BT 9.1 % and Am-BIS-BT 5.2 % respectively, were due to the addition of HC and BT during the synthesis of these materials.

The SEM images of HC-g-Am-BIS-BT and Am-BIS-BT are shown in **Figure 6**.

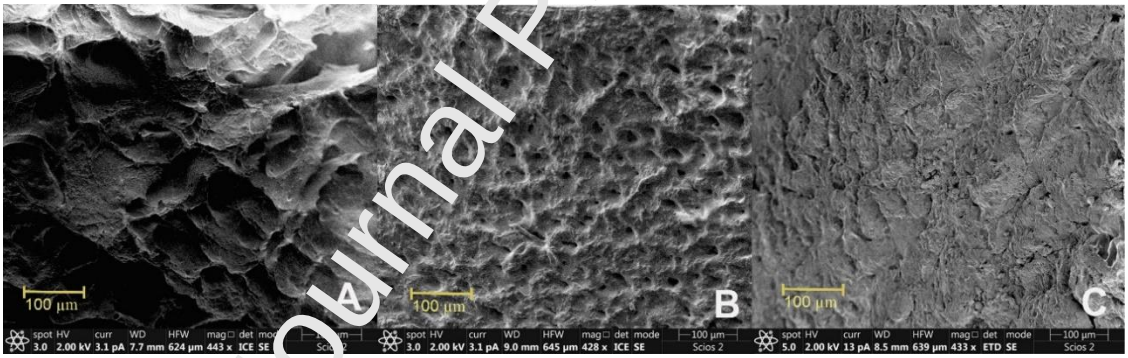

Figure 6. SEM images of **A:** Am-BIS-BT, **B:** HC-g-Am-1-BIS-BT and **C:** HC-g-Am-5-BIS-BT hydrogels.

The micrographs were showed in **Figures 6** (**A, B and C**). In all cases a uniform and regular network structure indicate that the reaction between the different reactive and covalent crosslinking sites is well dispersed in the hydrogel network.

After the addition of HC (**Figure 6B**), we can observe a reduction of the porosity in the structure. The porous reduction is attributed to the increase in intermolecular interactions by hydrogen bonding generated by HC, which favors its cross-linking in the semi-IPN network. An increase in crosslinking of 1 to 5%

(**Figure B** and **C**) promotes the formation of crossover points, generating a greatest decreases in the pore size of the material [50]. The different morphologies according to the addition of HC or crosslinking could explain the behaviors of swelling and dye adsorption.

The swelling capacity of hydrogels varies depending on the physicochemical characteristics of the material. The degree of swelling of the different samples recorded over time can be seen in **Figure 7**.

As regards the study of the effect of BIS concentration on swelling and its effect during crosslinked Am-BIS-BT was investigated (**Figure 7A**). BIS allows the formation of a cross-linked structure of the polymer networks, which prevents their dissolution in aqueous media. As can be seen in **Figure 7A**, when increasing the amount of BIS used in the synthesis, decreases in the absorption capacity of the material. Similar results were reported by Peng *et al.* in the synthesis of semi-IPNs with HC-g-poly(acrylic acid) who observed changes in the absorption capacity of the synthesized polymers from the variation of the crosslinking agent BIS. It is important to remark that the increase of the concentration of BIS produced an increased crosslinking point generated a decrease in the free spaces among the networks, consequently, the right 3D structure cannot hold a large quantity of water [51]. In addition, in the case of HC-g-Am-BIS, it can lead to new hydrogen bonds with the HC.

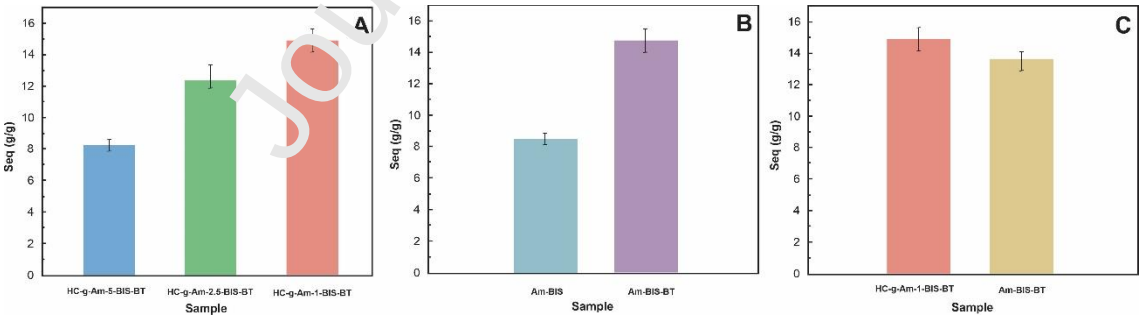

Figure 7 A: Effect of concentration of BIS; **B**: concentration of BT; and **C:** concentration of HC in swelling ratios of hydrogels.

Secondly, the BT effect on the water absorbency in the hydrogel was investigated and is observed in **Figure 7B**. The addition of BT generates an

increase in the absorption of water in the material. These results can be attribute to the integration of interpenetrated networks with the BT and they could be cross-linked through noncovalent bonding such as hydrogen bonding a resulting in a hydrogel 3D network formation [42]. These results were similar to those reported by Dai *et al* 2018, who attributed the increased swelling of hydrogels with BT to the formation of porous structures facilitating the diffusion of water in the material [36].

Finally, the HC effect on the swelling capacity of the gels is shown in **Figure 7C**. As previously observed, the decreasing effect in swelling of the materials with the highest percentage of BIS was attributed to increased cross-linking of the semi-IPN gels. In the case of the HC-g-Am-BIS-BT system, the slight increases the of the absorption S_{eq} (swelling at equilibrium), is due to HC acting as a multifunctional crosslinker through both covalent and hydrogen bonds between HC and Am-BIS-BT. Moreover, the physical interaction between HC and the Am-BIS network increases the effective crosslink density which can be attributed to entanglement and network interpenetration.

3.3 Adsorption study

For dye removal studies, samples with the best water absorbency HC-g-Am-1-BIS-BT and Am-BIS-BT were used to study the effect of HC on the adsorption of both cationic dyes (MB and Rh B) and the anionic azo dye (MR) at an initial concentration of 10-400 mg/L (**Figure 8**). The adsorption capacity of the hydrogels was determined at different contact times contact with the pigment models. The results showed that MB was removed after 1 h for Am-BIS-BT a 69.5%, while HC-Am-1-BIS-BT showed a major removal of the MB almost all initial concentrations of the MB (95.6 %) and it continuously increased with time until a plateau was reached at 10 h.

On the other hand, no significant differences were observed in the removal of the Rh B by the HC-Am-1-BIS-BT (49.7 %) and Am-BIS-BT (51.5 %) materials. This is because even though Rh B is a cationic dye like MB, it has a larger molecular structure which caused greater steric hindrance than MB when forming interactions with functional groups on a network of Am-BIS-BT during the adsorption process [52,53]. Regarding the adsorption studies carried out using

MR, was observed a low dye removal in both materials. This effect can be associated to the negative form of MR in a basic solution that generates a repulsion between MR and pendant groups in the materials, leading to a relatively low removal efficiency.

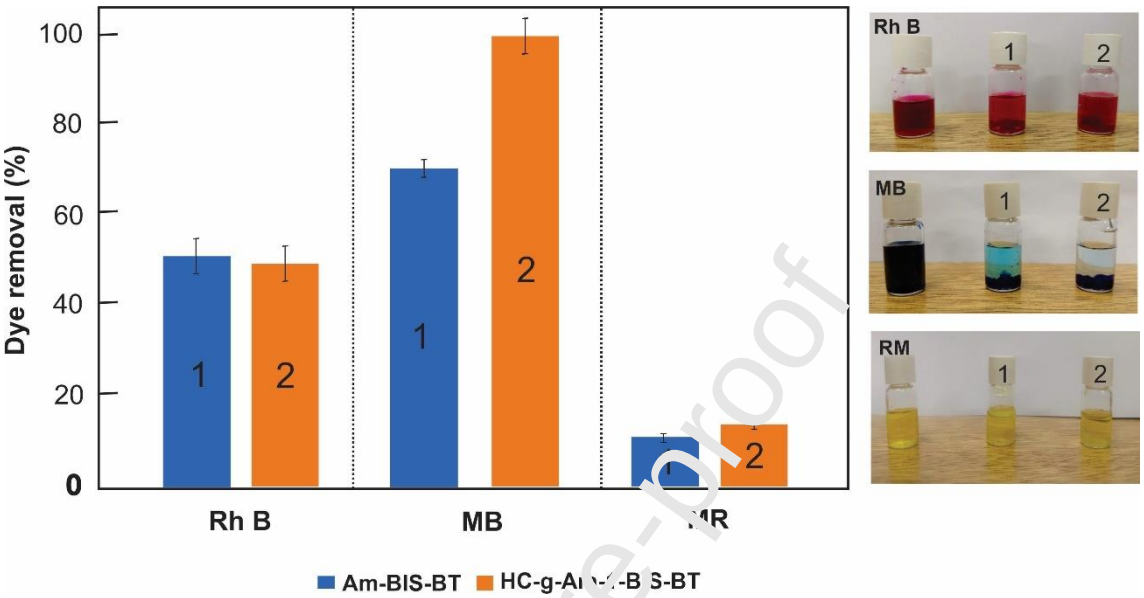

Figure 8. Dye removal percentage of MB, Rh B, and RM dyes by HC-g-Am-1-BIS-BT and Am-BIS-BT hydrogels.

Since the hydrogels showed the highest adsorption capacity towards MB, this dye was used for further studies of kinetics and adsorption behavior. In this sense compared the effect of the incorporation of HC in the network to understand the adsorption mechanism of MB on hydrogel, and to ascertain the rate of controllable step during the dyes adsorption process. In this case, the adsorption kinetic studies were investigated using pseudo-first-order (PFO) and pseudo-second-order (PSO) models.

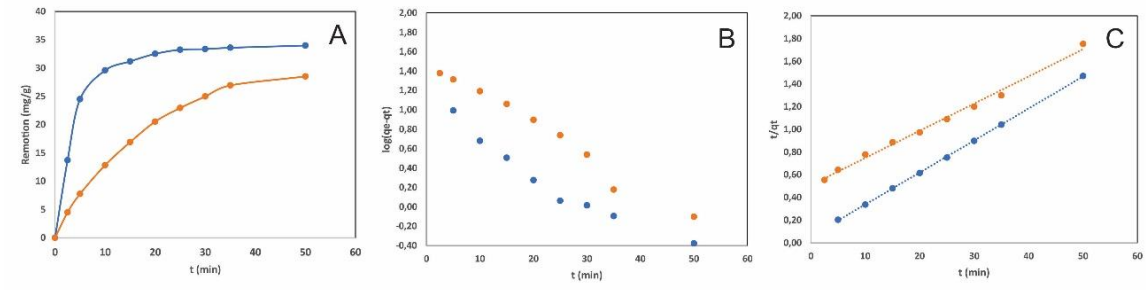

Figure 9. Removal percentage of HC-g-Am-BIS-BT and Am-BIS-BT at different A: contact times, B: plots of pseudo-first-order model, and C: pseudo second-order model adsorption.

centage of HC-g-Am-BIS-BT and Am-BIS-BT at different A: contact times, B: plots of pseudo-first-order model, and C: pseudo-second-order model adsorption.

Initially, the HC-g-Am-BIS-BT adsorption process was fast (**Figure 9A**), removing at around 95 % of MB at 60 min. After that, a slow adsorption was observed. This result was reported by Maijan *et al.* who obtained a behavior similar to elastic superabsorbent natural rubber/PAM hydrogel used to adsorbed cationic and anionic azo dyes. This research group, assign these results to the number of sites binding availability [53]. In the first 60 minutes exist a major greater number of active sites which enables a quick binding of adsorbate molecules onto MB. Later in the equilibrium state, the leftover active sites become progressively not capable of being occupied by the adsorbate due to the repulsive forces between the pollutant ions or molecules and the adsorbent, resulting in the formation of a plateau [54–56].

However, hydrogel without HC has slower adsorption kinetics, this can be attributed to the absence of OH and COOH. Convincingly, the carboxyl and hydroxyl groups not only have a crosslinked effect but also offer sufficient sites to block MB through intermolecular interactions as dipole-dipole H-bond, Yoshida H-bond and n-π interaction (or n-π electron donor-acceptor interactions) [57–61].

Concerning the results corresponding to the kinetics studies, were plotted following the PFO and PSO models are shown (**Figure 9(B-C)**). According to the resultant parameters, summarized in **Table 2**, the R^2 value obtained from the PSO model is higher and close to 1 than that of the PFO model. These results indicated that both systems (HC-g-Am-BIS-BT and Am-BIS-BT), and the kinetics behavior are described for a PSO model. This model is controlled by a chemisorption process that involving a rate-controlling step of electrostatic attraction between positive and negative charges on cationic dye molecules and polymer chains, respectively [62].

Table 2. Kinetic parameters for MB adsorption on HC-g-Am-BIS-BT and Am-BIS-B hydrogels.

		Pseudo-first order		**Pseudo-second order**	
	q_e(mg/g)	K_1(1/min)	R^2	K_2(1/min)	R^2
Am-BIS-BT	28.45	0.0046	0.7718	0.0262	0.9932
HC-g-Am-1-BIS-BT	34.41	0.0192	0.9357	0.1060	0.9998

On the other hand, was realized adsorption tests (**S1 and S2, Supplementary material**). These results exhibited similarities comportament to the showed in the kinetic studies. The adsorption amounts of MB increased significantly with the increase of initial MB concentration, and the adsorption capacities of HC-g-Am-BIS-BT and Am-BIS-BT, which was caused by the higher MB concentration lessening the mass transfer resistance of dye molecules from the aqueous phase to the solid phase.

For the binary system, three important isotherms, Langmuir, Freundlich and Temkin, were applied to fit the equilibrium data using the dye of major adsorption (MB) in the materials. The correlation coefficient values from the linear fitting of Langmuir, Freundlich and Temkin isotherms indicated that the experimental data obtained for HC-g-1-Am-BIS-BT and Am-BIS-BT hydrogels better fitted the Langmuir isotherm than the Freundlich and Temkin isotherms (**Figure 10** and **Table 3)**. These results indicate monolayer adsorption of MB on specific homogenous sites of the adsorbent and that all sites are equivalent and relatively homogeneous [63–65].

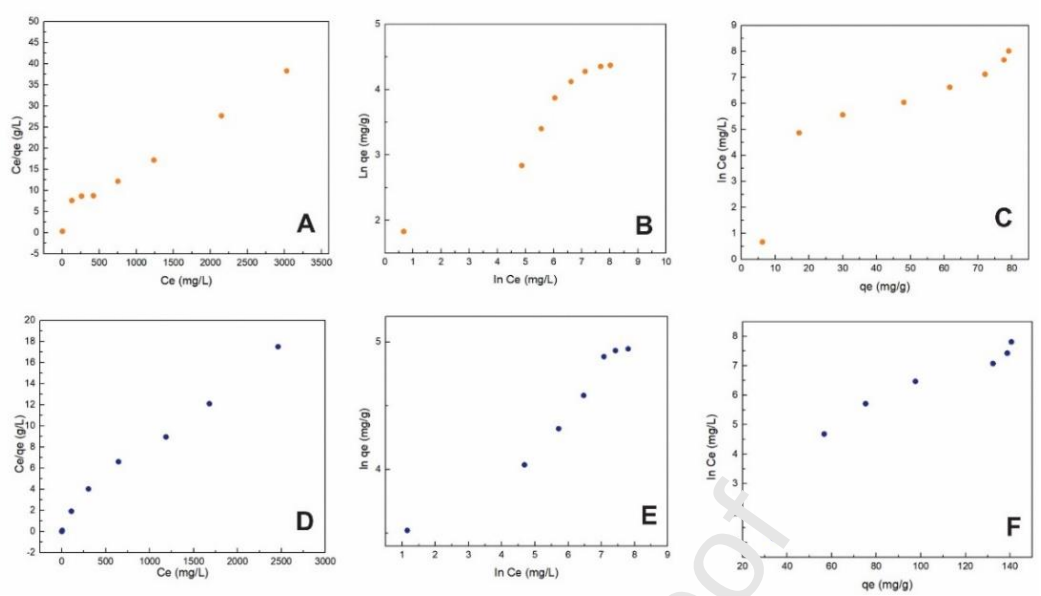

Figure 10. HC-g-Am-BIS-BT (**A-C**) and Am-BIS-BT (**D-F**). Plots of (**A** and **D**) Langmuir, (**B** and **E**) Freundlich isotherms and Tempkin isotherms (**C** and **F**).

An increase of q_{max} values from the Langmuir isotherm in the hydrogel with HC was observed (**Table 3**). The incorporation of HC in the system creates a densely cross-linked structure due to the formation of physical entanglement and hydrogen bonds. The chemical and physical cross-linking generated by the polymeric chains allow an increase in the interactions generated between them and MB, favoring their adsorption [53,58]. On the other hand, studies have shown a greater affinity towards natural HC and lignin because these biopolymer have acetylated groups that have been shown to significantly increase the adsorption capacity of cationic dyes [66–69].

These studies, in correlation with those of water absorption, coincide with the morphology observed by SEM. Obviously, the absorption of water is related to the pore size, which is not necessarily related to the adsorption of dyes. This is why there is an evident compromise between pore size and crosslinking to achieve optimal adsorption of this type of dye.

Table 3. Langmuir, Freundlich and Tempkin isotherms parameters for MB adsorption on HC-g-Am-BIS-BT and Am-BIS-BT hydrogels.

Dye	IPN	Langmuir isotherm model	Freundlich isotherm	Tempkin isotherm

		q_{max} (mg/g)b	K_L (L/mg)	R^2	1/n	K_f (mg/g)	R^2	B_T	K_T (L/mg)	R^2
MB	HC-g-Am-1-BIS-BT	140.66	7.34E-03	0,9833	0.221	23.222	0.9496	0.0492	8.60E+08	0.844
	Am-BIS-BT	88.495	2.95E-03	0.9792	0.376	4.2371	0.9442	0.0737	1.07E+13	0.8012

Also, separation factors (R_L) calculated at all initial concentrations lie within the range of 0–1, indicating that the adsorption of MB on the surface of hydrogels was favorable [70].

BET analysis was conducted on the samples revealing that the hydrogels prepared with and without hemicellulose showed specific surface areas of approximately 10.83 m^2/g and 5.79 m^2 g/g, respectively with average diameters pore corresponding to mesoporous material. These increases in the specific area confirm the results shown through the adsorption test and underscore the efficacy of employing hemicelluloses as a suitable approach for augmenting the adsorption capacity of the hydrogels.

FTIR-ATR analysis revealed possible interactions of the surface functional groups adsorbent and MB molecules (**Figure 11**).

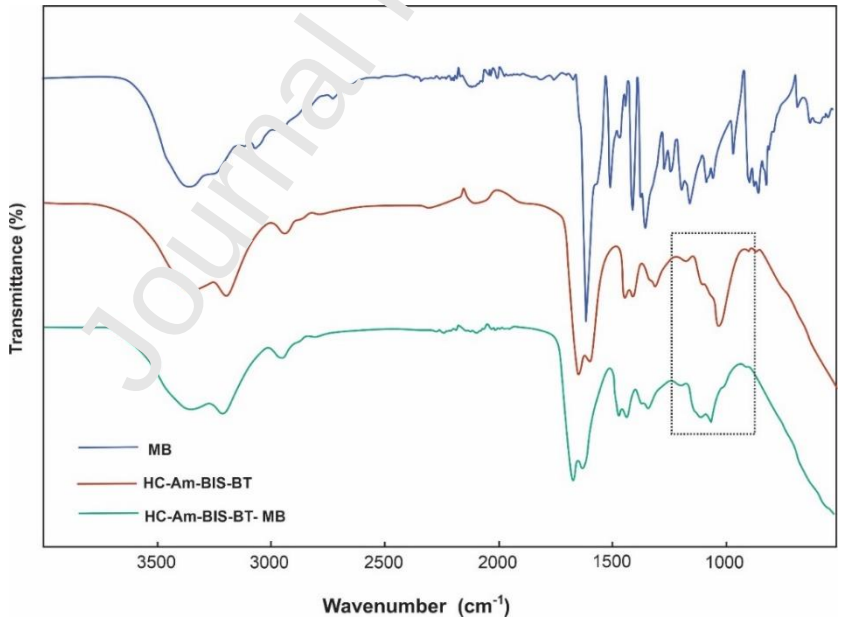

Figure 11. FTIR-ATR spectrum of HC-g-Am-1-BIS-BT before and after HC-g-Am-1-BIS-BT-MB contacting with MB.

Significant changes are observed between 1140-1030 cm^{-1} corresponding to the C-O stretching signal. These results are similar to those described by Makhado *et al* 2022 and Said *et al* 2022, who synthesized a hydrogel from ghatti

gum/polyacrylic acid/TiO_2 and microcellulose phosphorylated respectively, attributed this decrease to the formation of hydrogen bonds and electrostatic interactions during the adsorption process between MB and the adsorbent [71,72].

On the other hand, regeneration capability of the HC-g-Am-1-BIS-BT has been estimated by adsorption-desorption process from the MB solution of 400 mg/L (**Figure 12**). After being reused five times, HC-g-AM-BIS-BT shows a slight decrease in adsorption capacity. These results indicate the capacity of the new interpenetrate network suggesting the reusable ability for it is sustainable potential use for purification of dye-containing wastewater [73,74].

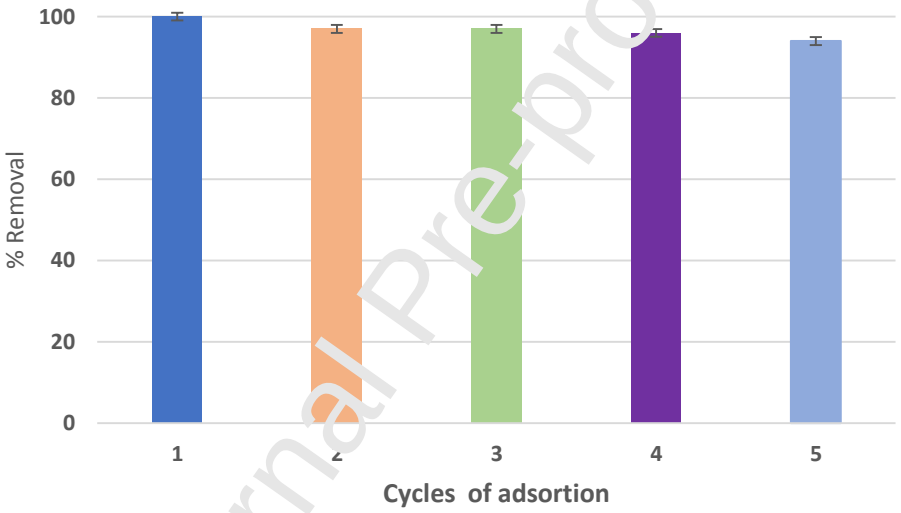

Figure 12. Adsorption studies capacities of the HC-g-AM-BIS-BT for MB after regenerated five times.

The maximum adsorption capacity (q_{max}) of HC-g-AM-BIS-BT as an adsorbent towards the removal of MB is compared with other literatures. (**Table 4**). Although the bentonite exhibits adsorption values akin to those of the material synthesized in this study, the literature substantiates the constrained retrieval of this substance from the liquid phase. Conversely, systems comprising networks of polysaccharides, crosslinked polymers, and clays displayed q_{max} values akin to those documented in this investigation. This finding affirms the synergistic impact of these systems. In contrast, the converse situation was observed concerning the material synthesized from xylan-gelatin.

Table 4: Comparative studies of MB dye with literature

Reference	Authors	Composition	pH	qmax
This Article	Rodríguez-Ramírez et al 2022	HC-g-Am-1-BIS-BT	7	140.7 mg/g
[75]	Pourjavadi et al 2016	Carrageenan-g-polyacrylamide/bentonite	7	156.3 mg/g
[76]	Hong et al 2009	Bentonite	7	151.0 mg/g
[77]	Cheng et al 2016	Cellulose/PVA/Fe_3O_4	7	71.1 mg/g

4. Conclusions

In summary, semi-interpenetrating polymer network hydrogels were efficiently prepared from HC provided of endemic Argentinean plant, crosslinked BIS and BT. The methodology applied allows to reduce by 10 % the use of monomers derived from petroleum and therefore reduces production costs by using a waste product. It is important to note that HC hydrogels have similar water absorption performance to those without HC. Also, a hydrogel with HC can be used to remove dyes, such as rhodamine B, methylene blue and methylene red. It is important to remark that the highest removal was obtained with methylene blue. This adsorption was monolayer on a homogeneous surface and was controlled by physisorption and chemisorption. The new semi-interpenetrated network can remove almost 100% of methylene blue within 60 min, with a maximum adsorption capacity of 140.66 mg/g, being able to use five adsorption-desorption sequences with a high adsorption rate. In the future, this network semi-IPN will be studied by increasing the proportion of biopolymer. In the other hand sewage treatment can be carried out to adsorb heavy metal ions, pharmaceutical and their metabolites.

5. Acknowledgment

NLG and NBD are research members of the National Council of Research and Technology (CONICET, Argentina). The authors thank University of Buenos Aires,

This work was financially supported by University of Buenos Aires (UBACyT20020170100090BA), CONICET (PIP 2021–2023, code 11220200100993CO) and the Ministry of Science and technology of Argentina (MINCYT, PICT-2020-SERIEA-00710). CARR is a doctoral scholarship from CONICET and JET is postdoctoral scholarship from YTEC-CONICET. The authors thank Dr. Alberto Caneiro for SEM images.

References

[1] K. Roa, E. Oyarce, G.D.C. Pizarro, S. Julio, Lignocellulose-based materials and their application in the removal of dyes from water : A review, Sustain. Mater. Technol. 29 (2021). https://doi.org/10.1016/j.susmat.2021.e00320.

[2] T. Liu, C.O. Aniagor, M.I. Ejimofor, M.C. Menkiti, Y.M. Wakawa, J. Li, R.A. Akbour, P.-S. Yap, S.Y. Lau, J. Jeevanandam, Recent developments in the utilization of modified graphene oxide to adsorb dyes from water: A review, J. Ind. Eng. Chem. 117 (2022) 21–37. https://doi.org/10.1016/j.jiec.2022.10.008.

[3] K. Sadanand Pandey, Edwin Makhado, Sujeong Kim, Misook, Recent developments of polysaccharide based superabsorbent nanocomposite for organic dye contamination removal from wastewater, Environ. Res. (2022) 109181. https://doi.org/10.1016/j.buildenv.2022.109181.

[4] A. Sridhar, M. Ponnuchamy, A. Kapoor, S. Prabhakar, Valorization of food waste as adsorbents for toxic dye removal from contaminated waters : A review, J. Hazard. Mater. 424 (2022) 127432. https://doi.org/10.1016/j.jhazmat.2021.127432.

[5] M.D. Lord, G. Neve, M. Keating, J. Budhathoki-Uprety, Polycarbodiimide for Textile Dye Removal from Contaminated Water, ACS Appl. Polym. Mater. 4 (2022) 6192–6201. https://doi.org/10.1021/acsapm.2c00959.

[6] D. Peramune, D.C. Manatunga, R.S. Dassanayake, V. Premalal, R.N. Liyanage, C. Gunathilake, N. Abidi, Recent advances in biopolymer-based advanced oxidation processes for dye removal applications: A review, Environ. Res. 215 (2022) 114242. https://doi.org/10.1016/j.envres.2022.114242.

[7] R. Sivakumar, N.Y. Lee, Adsorptive removal of organic pollutant methylene

blue using polysaccharide-based composite hydrogels, Chemosphere. 286 (2022) 131890. https://doi.org/10.1016/j.chemosphere.2021.131890.

[8] A. Ahmad, S.H. Mohd-Setapar, C.S. Chuong, A. Khatoon, W.A. Wani, R. Kumar, M. Rafatullah, Recent advances in new generation dye removal technologies: Novel search for approaches to reprocess wastewater, RSC Adv. 5 (2015) 30801–30818. https://doi.org/10.1039/c4ra16959j.

[9] T.A. Aragaw, F.M. Bogale, Biomass-Based Adsorbents for Removal of Dyes From Wastewater : A Review, Front. Environ. Sci. 9 (2021). https://doi.org/10.3389/fenvs.2021.764958.

[10] S. Pandey, E. Makhado, S. Kim, M. Kang, Recent developments of polysaccharide based superabsorbent nanocomposite for organic dye contamination removal from wastewater – A review, Environ. Res. 217 (2023) 114909. https://doi.org/10.1016/j.envres.2022.114909.

[11] S. Kim, A.U. Regitsky, J. Song, N. Holten-andersen, J. Ilavsky, G.H. Mckinley, In situ mechanical reinforcement of polymer hydrogels via metal-coordinated crosslink mineralization, Nat. Commun. (2021) 1–10. https://doi.org/10.1038/s41467-021-20953-7.

[12] D. Properties, N. Martin, G. Youssef, Dynamic Properties of Hydrogels and Fiber-reinforced Hydrogels, J. Mech. Behav. Biomed. Mater. (2018). https://doi.org/10.1016/j.jmbbm.2018.06.008.

[13] A. Agrawal, N. Rahbar, P.D. Calvert, Strong fiber-reinforced hydrogel, Acta Biomater. 9 (2013) 5313–5318. https://doi.org/10.1016/j.actbio.2012.10.011.

[14] M. Ahmadian, M. Jaymand, Interpenetrating polymer network hydrogels for removal of synthetic dyes : A comprehensive review, Coord. Chem. Rev. 486 (2023) 215152. https://doi.org/10.1016/j.ccr.2023.215152.

[15] R. Article, Y. Lu, Q. He, G. Fan, Q. Cheng, G. Song, Extraction and modi fi cation of hemicellulose from lignocellulosic biomass : A review, Green Process. Synth. (2021) 779–804.

[16] W. Wang, J. Wang, Y. Zhao, H. Bai, M. Huang, T. Zhang, S. Song, High-

performance two-dimensional montmorillonite supported-poly(acrylamide-co-acrylic acid) hydrogel for dye removal, Environ. Pollut. (2019) 113574. https://doi.org/10.1016/j.envpol.2019.113574.

[17] X. Fu, H. Zhuang, K.R. Reddy, N. Jiang, Y. Du, Novel composite polymer-amended bentonite for environmental containment : Hydraulic conductivity , chemical compatibility , enhanced rheology and polymer stability, Constr. Build. Mater. 378 (2023) 131200. https://doi.org/10.1016/j.conbuildmat.2023.131200.

[18] Z. Huang, Y. Li, W. Chen, J. Shi, N. Zhang, X. Wang, Z. Li, L. Gao, Y. Zhang, Modified bentonite adsorption of organic pollutants of dye wastewater, Mater. Chem. Phys. 202 (2017) 266–276. https://doi.org/10.1016/j.matchemphys.2017.09.028.

[19] K. Sanavada, M. Shah, D. Gandhi, A. Unnarkat, P. Vaghasiya, Environmental Nanotechnology , Monitoring & Management A systematic and comprehensive study of Eco-friendly bentonite clay application in esterification and wastewater treatment, Environ. Nanotechnology, Monit. Manag. 20 (2023) 100784. https://doi.org/10.1016/j.enmm.2023.100784.

[20] G. Sennakesavan, M. Mostakhdemin, L.K. Dkhar, A. Seyfoddin, S.J. Fatihhi, Acrylic acid / acrylamide based hydrogels and its properties - A review, Polym. Degrad. Stab. 180 (2020) 109308. https://doi.org/10.1016/j.polymdegradstab.2020.109308.

[21] J. Kwei, C. Wei, M. Rafie, S. Seng, W. Wei, Recent advances of modified polyacrylamide in drilling technology, J. Pet. Sci. Eng. 215 (2022) 110566. https://doi.org/10.1016/j.petrol.2022.110566.

[22] M. Jiang, N. Niu, L. Chen, A template synthesized strategy on bentonite-doped lignin hydrogel spheres for organic dyes removal, Sep. Purif. Technol. 285 (2022) 120376. https://doi.org/10.1016/j.seppur.2021.120376.

[23] G.L. Dotto, F.K. Rodrigues, E.H. Tanabe, R. Fröhlich, D.A. Bertuol, T.R. Martins, E.L. Foletto, Journal of Environmental Chemical Engineering Development of chitosan / bentonite hybrid composite to remove hazardous anionic and cationic dyes from colored ef fl uents, J. Environ. Chem. Eng. 4 (2016) 3230–

3239. https://doi.org/10.1016/j.jece.2016.07.004.

[24] C. A. Rodríguez Ramírez, M. Fascio, R. Agusti, N.B. D'Accorso, N.L. Garcia, Eco-friendly and efficient modification of native hemicelluloses via click reactions, New J. Chem. (2023). https://doi.org/DOI https://doi.org/10.1039/D2NJ04076J.

[25] C.A. Rodríguez-ramírez, A. Dufresne, N.D. Accorso, N. Lis, International Journal of Biological Macromolecules Alternative modification by grafting in bamboo cellulose nanofibrils : A potential option to improve compatibility and tunable surface energy in bionanocomposites, Int. J. Biol. Macromol. 211 (2022) 626–638. https://doi.org/10.1016/j.ijbiomac.2022.05.050.

[26] S. Rajoriya, V.K. Saharan, A.S. Pundir, M. Nigam, K. Roy, Adsorption of methyl red dye from aqueous solution onto eggshell waste material: Kinetics, isotherms and thermodynamic studies, Curr. Res. Green Sustain. Chem. 4 (2021) 100180. https://doi.org/10.1016/j.crgsc.2021.100180.

[27] K.C. Bedin, A.C. Martins, A.L. Cazetta, O. Pezoti, V.C. Almeida, KOH-activated carbon prepared from sucrose spherical carbon: Adsorption equilibrium, kinetic and thermodynamic studies for Methylene Blue removal, Chem. Eng. J. 286 (2016) 476–484. https://doi.org/10.1016/j.cej.2015.10.099.

[28] D.R. Biswal, R.P. Singh, Characterisation of carboxymethyl cellulose and polyacrylamide graft copolymer, Carbohydr. Polym. 57 (2004) 379–387. https://doi.org/10.1016/j.carbpol.2004.04.020.

[29] W. Wang, S. Yang, A. Zhang, Z. Yang, Preparation and properties of novel corn straw cellulose–based superabsorbent with water-retaining and slow-release functions, J. Appl. Polym. Sci. 137 (2020) 1–12. https://doi.org/10.1002/app.48951.

[30] D. Qiao, L. Yu, X. Bao, B. Zhang, F. Jiang, Understanding the microstructure and absorption rate of starch-based superabsorbent polymers prepared under high starch concentration, Carbohydr. Polym. 175 (2017) 141–148. https://doi.org/10.1016/j.carbpol.2017.07.071.

[31] C. Zhou, Q. Wu, Colloids and Surfaces B : Biointerfaces A novel polyacrylamide nanocomposite hydrogel reinforced with natural chitosan

nanofibers, Colloids Surfaces B Biointerfaces. 84 (2011) 155–162. https://doi.org/10.1016/j.colsurfb.2010.12.030.

[32] J.L. Wen, L.P. Xiao, Y.C. Sun, S.N. Sun, F. Xu, R.C. Sun, X.L. Zhang, Comparative study of alkali-soluble hemicelluloses isolated from bamboo (Bambusa rigida), Carbohydr. Res. 346 (2011) 111–120. https://doi.org/10.1016/j.carres.2010.10.006.

[33] J. Zhu, F. Guo, C. Ma, H. Wang, J. Wen, Y. Yu, Industrial Crops & Products The alkaline extraction efficiency of bamboo cell walls is related to their structural differences on both anatomical and molecular level, Ind. Crop. Prod. 178 (2022) 114628. https://doi.org/10.1016/j.indcrop.2022.114628.

[34] K. li Wang, B. Wang, R. Hu, X. Zhao, H. Li, G. Zhou, L. Song, A. min Wu, Characterization of hemicelluloses in Phyllostachys edulis (moso bamboo) culm during xylogenesis, Carbohydr. Polym. 221 (2019) 127–136. https://doi.org/10.1016/j.carbpol.2019.05.088.

[35] H. Dai, H. Huang, Synthesis , characterization and properties of pineapple peel cellulose- g -acrylic acid hydrogel loaded with kaolin and sepia ink, Cellulose. 24 (2017) 69–84. https://doi.org/10.1007/s10570-016-1101-0.

[36] H. Dai, Y. Huang, H. Huang, Eco-friendly polyvinyl alcohol/carboxymethyl cellulose hydrogels reinforced with graphene oxide and bentonite for enhanced adsorption of methylene blue, Elsevier Ltd., 2018. https://doi.org/10.1016/j.carbpol.2017.12.073.

[37] S. Thakur, A. Verma, V. Kumar, X. Jin Yang, S. Krishnamurthy, F. Coulon, V.K. Thakur, Cellulosic biomass-based sustainable hydrogels for wastewater remediation: Chemistry and prospective, Fuel. 309 (2022) 122114. https://doi.org/10.1016/j.fuel.2021.122114.

[38] S. Ihaddaden, D. Aberkane, A. Boukerroui, D. Robert, Journal of Water Process Engineering Removal of methylene blue (basic dye) by coagulation-flocculation with biomaterials (bentonite and Opuntia ficus indica), J. Water Process Eng. 49 (2022) 102952. https://doi.org/10.1016/j.jwpe.2022.102952.

[39] X.F. Sun, Z. Jing, G. Wang, Preparation and swelling behaviors of porous

hemicellulose-g-polyacrylamide hydrogels, J. Appl. Polym. Sci. 128 (2013) 1861–1870. https://doi.org/10.1002/app.38240.

[40] X. Yu, X. Huang, C. Bai, X. Xiong, Modification of microcrystalline cellulose with acrylamide under microwave irradiation and its application as flocculant, Environ. Sci. Pollut. Res. 26 (2019) 32859–32865. https://doi.org/10.1007/s11356-019-06317-1.

[41] B. Kalkan, N. Orakdogen, Negatively charged poly(N-isopropyl acrylamide-co-methacrylic acid)/polyacrylamide semi-IPN hydrogels: Correlation between swelling and compressive elasticity, React. Funct. Polym. 174 (2022) 105245. https://doi.org/10.1016/j.reactfunctpolym.2022.105245.

[42] X. Liu, M. Chang, H. Zhang, J. Ren, Reinforcement Effects of Inorganic Nanoparticles for PAM- g -carboxymethyl Xylan Nanocomposite Hydrogels, Macromol. Mater. Eng. 2200251 (2022) 1–13. https://doi.org/10.1002/mame.202200251.

[43] W. Zhao, L. Glavas, K. Odelius, U. Edlund, A.C. Albertsson, A robust pathway to electrically conductive hemicellulose hydrogels with high and controllable swelling behavior, Polymer (Guildf). 55 (2014) 2967–2976. https://doi.org/10.1016/j.polymer.2014.05.003.

[44] W. Liu, Q. Hou, C. Mao, Z. Yuan, K. Li, Hemicelluloses Prior to Aspen Chemithermomechanical Pulping: Pre- Extraction, Separation, and Characterization, Journa Agric. Food Chem. (2012). https://doi.org/dx.doi.org/10.1021/jf300787b.

[45] P. Peng, F. Peng, J. Bian, F. Xu, R.C. Sun, J.F. Kennedy, Isolation and structural characterization of hemicelluloses from the bamboo species Phyllostachys incarnata Wen, Carbohydr. Polym. 86 (2011) 883–890. https://doi.org/10.1016/j.carbpol.2011.05.038.

[46] C. Nakason, T. Wohmang, A. Kaesaman, S. Kiatkamjornwong, Preparation of cassava starch-graft-polyacrylamide superabsorbents and associated composites by reactive blending, Carbohydr. Polym. 81 (2010) 348–357. https://doi.org/10.1016/j.carbpol.2010.02.030.

[47] X. Liu, S. Luan, W. Li, Utilization of waste hemicelluloses lye for

superabsorbent hydrogel synthesis, Int. J. Biol. Macromol. 132 (2019) 954–962. https://doi.org/10.1016/j.ijbiomac.2019.04.041.

[48] H. Hosseinzadeh, M. Sadeghzadeh, M. Babazadeh, Preparation and Properties of Carrageenan- g -Poly (Acrylic Acid)/ Bentonite Superabsorbent Composite, J. Biomater. Nanobiotechnol. 2011 (2011) 311–317. https://doi.org/10.4236/jbnb.2011.23038.

[49] J.-L. Ren, R.-C. Sun, Hemicelluloses, 1st ed., Elsevier, 2010. https://doi.org/10.1016/B978-0-444-53234-3.00004-3.

[50] J.S. Gonzalez, A. Ponce, V.A. Alvarez, Preparation and Characterization of Poly (Vinylalcohol)/Bentonite Hydrogels for Potential Wound Dressings, Adv. Mater. Lett. 7 (2016) 979–985. https://doi.org/10.5185/amlett.2016.6888.

[51] X.W. Peng, J.L. Ren, L.X. Zhong, F. Peng, R.C. Sun, Xylan-rich hemicelluloses-graft -acrylic acid ionic hydrogels with rapid responses to pH, salt, and organic solvents, J. Agric. Food Chem. 59 (2011) 8208–8215. https://doi.org/10.1021/jf201529y.

[52] S. Vahedi, O. Tavakoli, M. Khoobi, A. Ansari, M. Ali Faramarzi, Application of novel magnetic β-cyclodextrin anhydride polymer nano-adsorbent in cationic dye removal from aqueous solution, J. Taiwan Inst. Chem. Eng. 80 (2017) 452–463. https://doi.org/10.1016/j.jtice.2017.07.039.

[53] P. Maijan, K. Junlapong, J. Arayaphan, C. Khaokong, S. Chantarak, Synthesis and characterization of highly elastic superabsorbent natural rubber/polyacrylamide hydrogel, Polym. Degrad. Stab. 186 (2021). https://doi.org/10.1016/j.polymdegradstab.2021.109499.

[54] Y. Zhou, M. Zhang, Response to "Comment on 'removal of Crystal Violet by a Novel Cellulose-Based Adsorbent: Comparison with Native Cellulose,'" Ind. Eng. Chem. Res. 55 (2016) 1148. https://doi.org/10.1021/acs.iecr.5b04874.

[55] I. Ayouch, I. Kassem, Z. Kassab, I. Barrak, A. Barhoun, J. Jacquemin, K. Draoui, M. El Achaby, Crosslinked carboxymethyl cellulose-hydroxyethyl cellulose hydrogel films for adsorption of cadmium and methylene blue from aqueous solutions, Surfaces and Interfaces. 24 (2021) 101124. https://doi.org/10.1016/j.surfin.2021.101124.

[56] E.R. Kenawy, H. Tenhu, S.A. Khattab, A.A. Eldeeb, M.M. Azaam, Highly efficient adsorbent material for removal of methylene blue dye based on functionalized polyacrylonitrile, Eur. Polym. J. 169 (2022) 111138. https://doi.org/10.1016/j.eurpolymj.2022.111138.

[57] A. gamal El-Shamy, Novel in-situ synthesis of nano-silica (SiO2) embedded into polyvinyl alcohol for dye removal: Adsorption and photo-degradation under visible light, Polymer (Guildf). 242 (2022) 124579. https://doi.org/10.1016/j.polymer.2022.124579.

[58] S.D.K. Seera, D. Kundu, P. Gami, P.K. Naik, T. Banerjee, Synthesis and characterization of xylan-gelatin cross-linked reusable hydrogel for the adsorption of methylene blue, Carbohydr. Polym. 256 (2021) 117520. https://doi.org/10.1016/j.carbpol.2020.117520.

[59] L. Chen, Y. Zhu, Y. Cui, R. Dai, Z. Shan, H. Chen, Fabrication of starch-based high-performance adsorptive hydrogels using a novel effective pretreatment and adsorption for cationic methylene blue dye: Behavior and mechanism, Chem. Eng. J. 405 (2021) 126953. https://doi.org/10.1016/j.cej.2020.126953.

[60] P. Kongseng, P. Amornpitoksuk, S. Chantarak, Development of multifunctional hydrogel composite based on poly(vinyl alcohol-g-acrylamide) for removal and photocatalytic degradation of organic dyes, React. Funct. Polym. 172 (2022) 105207. https://doi.org/10.1016/j.reactfunctpolym.2022.105207.

[61] J. Rana, G. Goindi, N. Kaur, S. Krishna, A. Kakati, Synthesis and application of cellulose acetate-acrylic acid-acrylamide composite for removal of toxic methylene blue dye from aqueous solution, J. Water Process Eng. 49 (2022) 103102. https://doi.org/10.1016/j.jwpe.2022.103102.

[62] K. Junlapong, P. Maijan, C. Chaibundit, S. Chantarak, Effective adsorption of methylene blue by biodegradable superabsorbent cassava starch-based hydrogel, Int. J. Biol. Macromol. 158 (2020) 258–264. https://doi.org/10.1016/j.ijbiomac.2020.04.247.

[63] B.C. Melo, F.A.A. Paulino, V.A. Cardoso, A.G.B. Pereira, A.R. Fajardo, F.H.A.

Rodrigues, Cellulose nanowhiskers improve the methylene blue adsorption capacity of chitosan-g-poly(acrylic acid) hydrogel, Carbohydr. Polym. 181 (2018) 358–367. https://doi.org/10.1016/j.carbpol.2017.10.079.

[64] B. Gao, H. Yu, J. Wen, H. Zeng, T. Liang, F. Zuo, C. Cheng, Super-adsorbent poly(acrylic acid)/laponite hydrogel with ultrahigh mechanical property for adsorption of methylene blue, J. Environ. Chem. Eng. 9 (2021) 106346. https://doi.org/10.1016/j.jece.2021.106346.

[65] C. Wang, G. Zhou, X. Wang, J. Liu, D. Li, C. Wu, Composite hydrogel membrane with high mechanical strength for treatment of dye pollutant, Sep. Purif. Technol. 275 (2021) 119154. https://doi.org/10.1016/j.seppur.2021.119154.

[66] C.H. Chan, C.H. Chia, S. Zakaria, M.S. Sajab, S.X. Chin, Cellulose nanofibrils: A rapid adsorbent for the removal of methylene blue, RSC Adv. 5 (2015) 18204–18212. https://doi.org/10.1039/c4ra15754k.

[67] B.N. Shelke, M.K. Jopale, A.H. Kategaonkar, Exploration of biomass waste as low cost adsorbents for removal of methylene blue dye: A review, J. Indian Chem. Soc. 99 (2022) 100530. https://doi.org/10.1016/j.jics.2022.100530.

[68] L. Liu, Z.Y. Gao, X.P. Su, X. Chen, L. Jiang, J.M. Yao, Adsorption removal of dyes from single and binary solutions using a cellulose-based bioadsorbent, ACS Sustain. Chem. Eng. 3 (2015) 432–442. https://doi.org/10.1021/sc500848m.

[69] B. Du, Y. Bai, Z. Pan, J. Xu, Q. Wang, X. Wang, G. Lv, J. Zhou, pH fractionated lignin for the preparation of lignin-based magnetic nanoparticles for the removal of methylene blue dye, Sep. Purif. Technol. 295 (2022) 121302. https://doi.org/10.1016/j.seppur.2022.121302.

[70] J. Arayaphan, P. Maijan, P. Boonsuk, S. Chantarak, Synthesis of photodegradable cassava starch-based double network hydrogel with high mechanical stability for effective removal of methylene blue, Int. J. Biol. Macromol. 168 (2021) 875–886. https://doi.org/10.1016/j.ijbiomac.2020.11.166.

[71] E. Makhado, B.R. Motshabi, D. Allouss, K.E. Ramohlola, K.D. Modibane, M.J.

Hato, R.M. Jugade, F. Shaik, S. Pandey, Development of a ghatti gum/poly (acrylic acid)/TiO2 hydrogel nanocomposite for malachite green adsorption from aqueous media: Statistical optimization using response surface methodology, Chemosphere. 306 (2022) 135524. https://doi.org/10.1016/j.chemosphere.2022.135524.

[72] H.A. Said, I. Ait Bourhim, A. Ouarga, I. Iraola-Arregui, M. Lahcini, A. Barroug, H. Noukrati, H. Ben youcef, Sustainable phosphorylated microcrystalline cellulose toward enhanced removal performance of methylene blue, Int. J. Biol. Macromol. (2022). https://doi.org/10.1016/j.ijbiomac.2022.11.172.

[73] F. Wang, Y. Zhu, W. Wang, L. Zong, T. Lu, A. Wang, Fabrication of CMC- g -PAM Superporous Polymer Monoliths via Eco-Friendly Pickering-MIPEs for Superior Adsorption of Methyl Violet and Methylene Blue, Front. Chem. 5 (2017) 1–13. https://doi.org/10.3389/fchem.2017.00033.

[74] Q. Lv, Y. Qiu, M. Wu, L. Wang, Poly (acrylic acid)/ poly (acrylamide) hydrogel adsorbent for removing methylene blue, (2020). https://doi.org/10.1002/app.49322.

[75] A. Pourjavadi, Z. Bassampour, H. Ghasemzadeh, M. Nazari, L. Zolghadr, S.H. Hosseini, Porous Carrageenan-g-polyacrylamide/bentonite superabsorbent composites: swelling and dye adsorption behavior, J. Polym. Res. 23 (2016) 1–10. https://doi.org/10.1007/s10965-016-0955-z.

[76] S. Hong, C. Wen, J. He, F. Gan, Y.S. Ho, Adsorption thermodynamics of Methylene Blue onto bentonite, J. Hazard. Mater. 167 (2009) 630–633. https://doi.org/10.1016/j.jhazmat.2009.01.014.

[77] Z. Wu, Q. Liao, P. Chen, D. Zhao, J. Huo, M. An, Y. Li, J. Wu, Z. Xu, B. Sun, M. Huang, Synthesis, characterization, and methylene blue adsorption of multiple-responsive hydrogels loaded with Huangshui polysaccharides, polyvinyl alcohol, and sodium carboxyl methyl cellulose, Int. J. Biol. Macromol. 216 (2022) 157–171. https://doi.org/10.1016/j.ijbiomac.2022.06.178.

Declaration of interests

☒The authors declare that they have no known competing financial interests or personal relationships that could have appeared to influence the work reported in this paper.

☐The authors declare the following financial interests/personal relationships which may be considered as potential competing interests:

.